Overflow Microfluidic Networks: Application to the Biochemical Analysis of Brain Cell Interactions in Complex Neuroinflammatory Scenarios

ARTICLE *in* ANALYTICAL CHEMISTRY · OCTOBER 2012

Impact Factor: 5.64 · DOI: 10.1021/ac302094z · Source: PubMed

8 AUTHORS, INCLUDING:

Fabio Bianco
Sanipedia srl
28 PUBLICATIONS **866** CITATIONS
SEE PROFILE

Ana Ruiz
European Commission
51 PUBLICATIONS **1,097** CITATIONS
SEE PROFILE

Michela Matteoli
University of Milan
138 PUBLICATIONS **7,839** CITATIONS
SEE PROFILE

analytical chemistry

Article

pubs.acs.org/ac

Overflow Microfluidic Networks: Application to the Biochemical Analysis of Brain Cell Interactions in Complex Neuroinflammatory Scenarios

Fabio Bianco,[*,†,¶] Noemi Tonna,[†,¶] Robert D. Lovchik,[‡] Rosa Mastrangelo,[†] Raffaella Morini,[§,∥] Ana Ruiz,[§,∥] Emmanuel Delamarche,[‡] and Michela Matteoli[∥,⊥]

[†]Neuro-Zone s.r.l., viale Ortles 22/4, 20139 Milano, Italy

[‡]IBM Research GmbH, Säumerstrasse 4, 8803 Rüschlikon, Switzerland

[§]Fondazione Filarete, viale Ortles 22/4, 20139 Milano, Italy

[∥]Department of Medical Biotechnology and Translational Medicine, University of Milano, Milano, Italy

[⊥]Humanitas Clinical and Research Center, Rozzano, Italy

ABSTRACT: Neuroinflammation plays a central role in neurodegenerative diseases and involves a large number of interactions between different brain cell types. Unraveling the complexity of cell−cell interaction in neuroinflammation is crucial for both clarifying the molecular mechanisms involved and increasing efficacy in drug development. Here, we provide a versatile analytical method for specifically addressing cell-to-cell communication, using primary brain cells, a microfluidic device, and a multiparametric readout approach. Different cell types are plated in separate chambers of a microfluidic network so that culturing conditions can be independently controlled and single cell types can be selectively primed with different stimuli. When chambers are microfluidically connected, the specific contribution of each cell type can be finely monitored by analyzing morphology, vitality, calcium dynamics, and electrophysiology parameters. We exemplify this approach by examining the role of astrocytes derived from two different brain regions (cortex and hippocampus) on neuronal viability in two types of neuroinflammatory insults, namely, metabolic stress and exposure to amyloid β fibrils, and demonstrate regional differences in glial control of neuronal physiopathology. In particular, we show that during metabolic stress, cortical but not hippocampal astrocytes play a neuroprotective role; also, in an exacerbated inflammatory scenario consisting in the exposure to Aβ + IL-1β, hippocampal but not cortical astrocytes play a detrimental role on neurons. Aside from bringing novel insights into the glial role in neuroinflammation, the method presented here represents a promising tool for addressing a wide range of biological and biochemical phenomena, characterized by a complex interaction of multiple cell types.

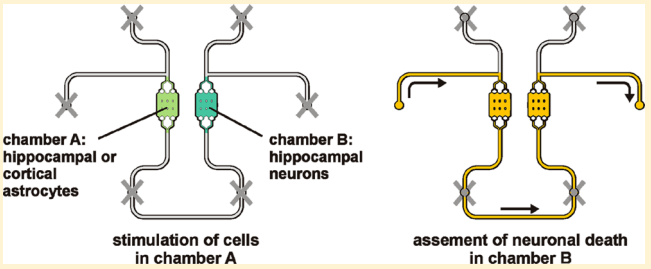

Neuroinflammation is a nonspecific immune reaction to tissue damage, neurodegeneration, or pathogen invasion, which occurs via the combined action of resident cells such as microglia and astrocytes and systemic cells like monocytes and macrophages.[1] It is widely established that the inflammatory response promoted by tissue damage serves to further engage the immune system, thus initiating tissue repair. Whereas in most cases this response is self-limiting and induces beneficial effects (e.g., phagocytosis of debris and apoptotic cells), sustained inflammation may result in tissue pathology, favoring the production of neurotoxic factors that amplify underlying disease states. In the latter case, the sustained inflammatory responses that contribute to neurodegeneration, although initially triggered in a disease-specific manner, may end up in becoming independent of the original inflammation-inducing molecules, such as amyloid-β (Aβ) in the case of Alzheimer's disease or metabolic alteration in the case of ischemia.[2]

Activation of astrocytes and microglia—the latter being the resident immune cells in the CNS—is one of the universal components of neuroinflammation, and crosstalk among these cells activate positive feedback loops, which may result in the amplification of inflammation. A large effort is therefore required to understand the cell-to-cell biochemical interactions underlying the neuroprotective or neurotoxic roles of microglia and astrocytes and how these interactions are perturbed in chronic disease states.[3]

Given the large number of possible combinatorial interactions between different brain cell types contributing to inflammations, and since cellular responses can be modulated by spatial and temporal signals from the surroundings,[4,5] there is a critical need for the identification of new strategies enabling cell-to-cell interactions to be addressed while manipulating cellular microenvironments. Microtechnology has provided tools to create microdevices for conducting many types of

Received: July 24, 2012
Accepted: October 24, 2012

   dx.doi.org/10.1021/ac302094z | *Anal. Chem.* XXXX, XXX, XXX−XXX

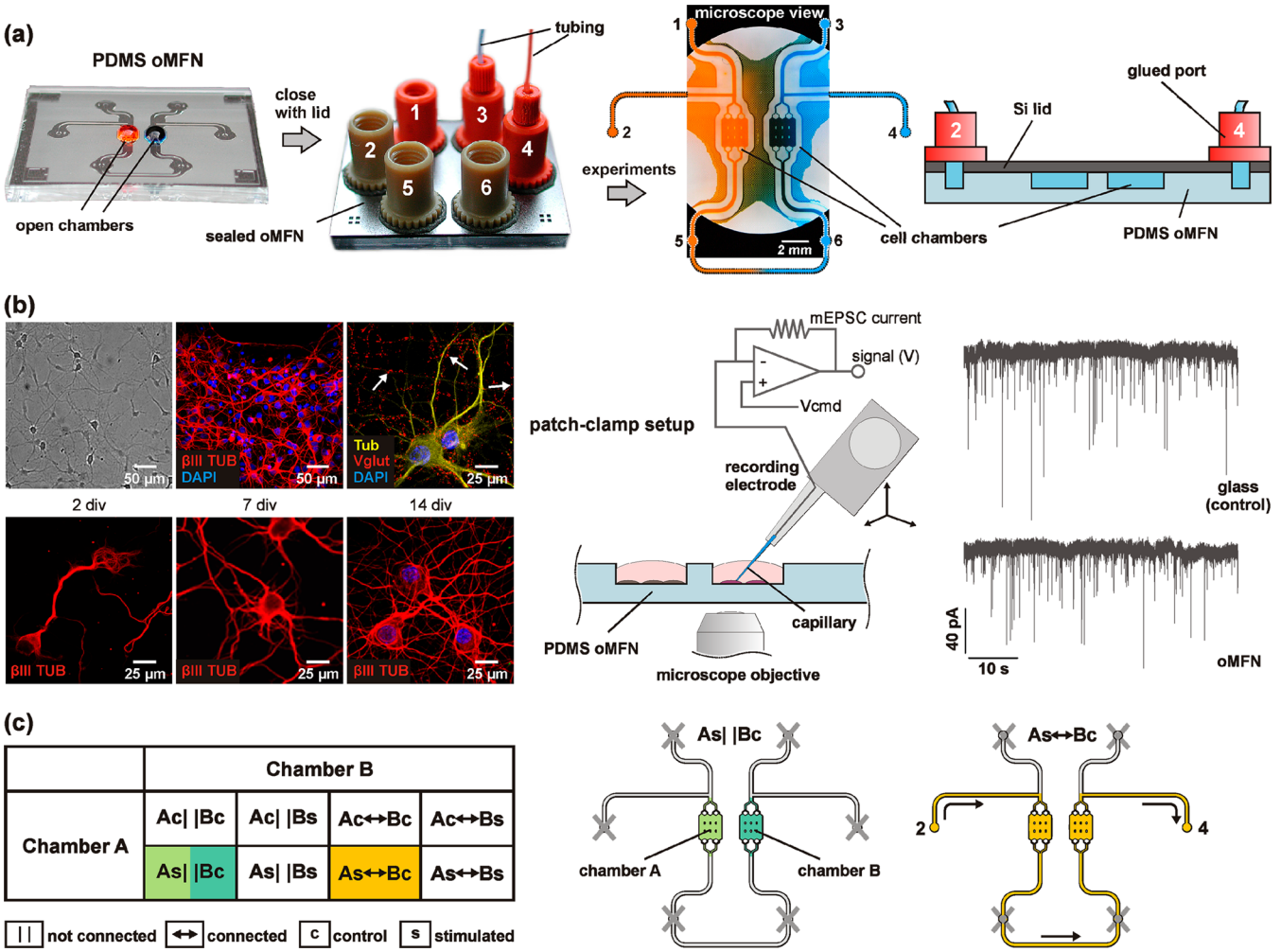

Figure 1. Illustration of an oMFN having two cell chambers, functional analysis of the cells in the chambers, and protocols for probing cells interactions. (a) Cell cultures can be grown independently, each with its own culturing medium, on the vicinal cell chambers of a oMFN made in PDMS. The oMFN can subsequently be closed using a lid at the appropriate culturing time. The wettable microstructures around the chambers wick away excess culture medium, guaranteeing perfect sealing and avoiding mixing of liquids. The six ports glued on the lid are in regard with microchannels servicing the chambers and can be left open, closed with a threaded plug, or connected to a computer-controlled syringe. For example, injecting a solution via port 2 while leaving port 4 open and the other ports closed results in perfusing both chambers one after the other. (b) Before closing the oMFN with a lid, cells can be extensively monitored as shown in these representative images of HNs grown on oMFNs. Cells differentiate in culture and express late-stage specific markers (i.e., Vglut), and staining with βIII tubulin shows development of the neuronal network. Moreover, representative traces of mEPSCs on HNs grown either under standard culturing conditions on glass or on oMFNs are shown. These traces exhibit comparable amplitude and frequency (see text for details). (c) Table and sketch showing experimental combinations for culturing and stimulating different cell populations plated in the chambers.

laboratory assays on a very small scale with cost and time savings and fine control of experimental setups. In particular, microfluidics have recently been used to study cellular ensembles as well as single cells.[6,7] Advantages of microfluidics over larger cell culture systems include the fact that few cells can be seeded, cultured, and studied in defined chemical and topographical environments.[8,9] However, most microfluidic devices lack flexibility, require complex protocols for cell deposition and maintenance in vitro, and do not allow a simultaneous analysis of morphological and real-time functional parameters. For example, microfluidics having multiple compartments for studying neurons and neuritic insults have been developed but it is difficult to keep one compartment independently stimulated from the other because the compartments are isolated by carefully maintaining an appropriate hydrostatic pressure between them.[10] In another example, a hand-held recirculation system was developed for culturing and imaging cells. This system includes many functionalities for seeding cells, pumping, and cell perfusion, but each cell culture requires one device and set of peripherals.[11] Here, we use overflow microfluidic networks (oMFNs)[12] for investigating various stress conditions on primary neurons, either in isolation or in microfluidic biochemical communication with glial cells. oMFNs have open cell chambers that are surrounded with array of wettable micropillars (i.e., "overflow zones"). These microfluidic chips therefore permit depositing and culturing cells for days and afterward closing the chambers with a lid for circulating precise amounts of chemicals/solutions throughout the chambers (see below). The general concept of seeding cells and studying them in open or closed chambers using microfluidics is broadly pursued.[13−15] Here, we specifically combine microfluidic-based experiments (i.e., culture and stimulation/stress of cells) with characterization methods such as immunocytochemical staining, quantitative intracellular

dx.doi.org/10.1021/ac302094z | Anal. Chem. XXXX, XXX, XXX−XXX

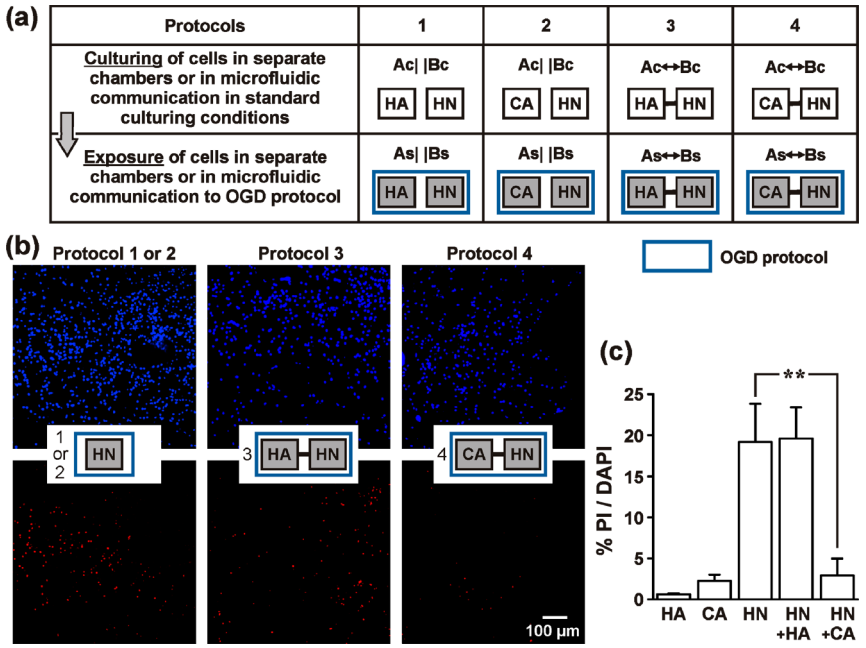

Figure 2. Effect of hippocampal (HAs) and cortical (CAs) astrocytes on neuronal viability during ischemic insult. (a) Representation of the experiments in which hippocampal neurons (HNs), grown independently or in microfluidic communication with either CAs or HAs, are challenged with oxygen−glucose deprivation (OGD) protocol. (b) Representative vitality images showing DAPI (blue)/PI (red) staining of HNs, grown either independently (protocols 1 and 2) or in microfluidic communication with either HAs (protocol 3) or CAs (protocol 4) and challenged with the OGD protocol. (c) Percentage of cell death following OGD protocol. Whereas challenged HAs and CAs do not exhibit increased cell death, challenged HNs show about 20% cell death. This number is significantly lower in OGD experiments that had HNs in microfluidic communication with CAs.

calcium imaging, and electrophysiological recordings, thus achieving a new method for efficiently dissecting specific cell type contribution. In addition, oMFNs are simple and disposable elements, which can be used with standard equipment such as cell incubators, syringe-based pumps, and inverted microscopes. Through this novel approach, we demonstrate that astrocytes from distinct brain regions differentially affect hippocampal neurons (HNs) challenged with different types of inflammatory stimuli.

RESULTS

Device Concept. The oMFNs used for all experiments presented here are made in poly(dimethylsiloxane) (PDMS). The oMFNs have a footprint of 32 × 26 mm^2, and the small separation distance of 1.6 mm between the chambers (edge-to-edge distance) allows visualization of both chambers simultaneously using a 4× microscope objective. The layout of the channels and corresponding ports permit liquids to be drawn sequentially or independently, if needed, through the chambers. The oMFNs are briefly treated with an oxygen-based plasma and coated with poly-L-lysine before a cell suspension is placed on each cell chamber. The overflow zones around the cell chambers have numerous wettable microstructures, which withdraw any excess liquid during the closing of the chip and ensure a sealing of the cells chambers. Figure 1a shows that different liquid droplets deposited on each cell chamber do not mix when the chip is closed. After sealing the oMFN with a Si lid, six ports are available for establishing specific culture or stimulating conditions by pumping media through the chambers with well-defined flow rates for the required time. For example, ports 1, 2, and 5 can be used to flush liquids through chamber A sequentially or in parallel so as to create a biochemical gradient in this chamber.[16] For flushing a chemical in both chambers, port 2 can be used while keeping ports 1, 3, 5, and 6 closed and port 4 open. The volume of each chamber is approximately 0.5 µL, thus minimizing the amount of cells required. Moreover, by using high-precision pumps with flow rates ranging from 10 to 50 nL s^{-1} very small amounts of reagents or culture media can be drawn through the cell chambers.

For the experiments described in this study, primary HNs from E18 rat embryos were seeded in a cell chamber and cultured for up to 10 days in vitro (DIV) before seeding primary astrocytes from P2 pups in the other chamber. Cell-containing oMFNs can be placed in an incubator, and the medium can conveniently be exchanged by pipetting as much and often as required before performing experiments. Figure 1b shows the different combinations of distinct cell populations plated in the chambers, the cell chamber connectivity, and the modalities of cell stimulation used in the present study. Cells can be grown in chambers either separately (||) or while being in microfluidic communication (↔). One cell population can be separately challenged with specific stimuli for a desired duration while the other cell population is kept perfused with culture medium (i.e., As||Bc) and then put into microfluidic communication for the required experimental time (i.e., As↔Bc). Alternatively, cells can be challenged while in microfluidic communication, thus enabling analysis of functional effects produced by soluble factors and/or organelles released from cells cultured in chamber A on target cells in chamber B. Target cells can be regularly inspected and assessed in terms of morphological/functional properties using standard optical, fluorescence, and electrophysiological characterization methods.

Functional Properties of Neurons Grown on oMFNs or in Standard Cultures. Primary HNs plated on oMFNs

dx.doi.org/10.1021/ac302094z | Anal. Chem. XXXX, XXX, XXX−XXX

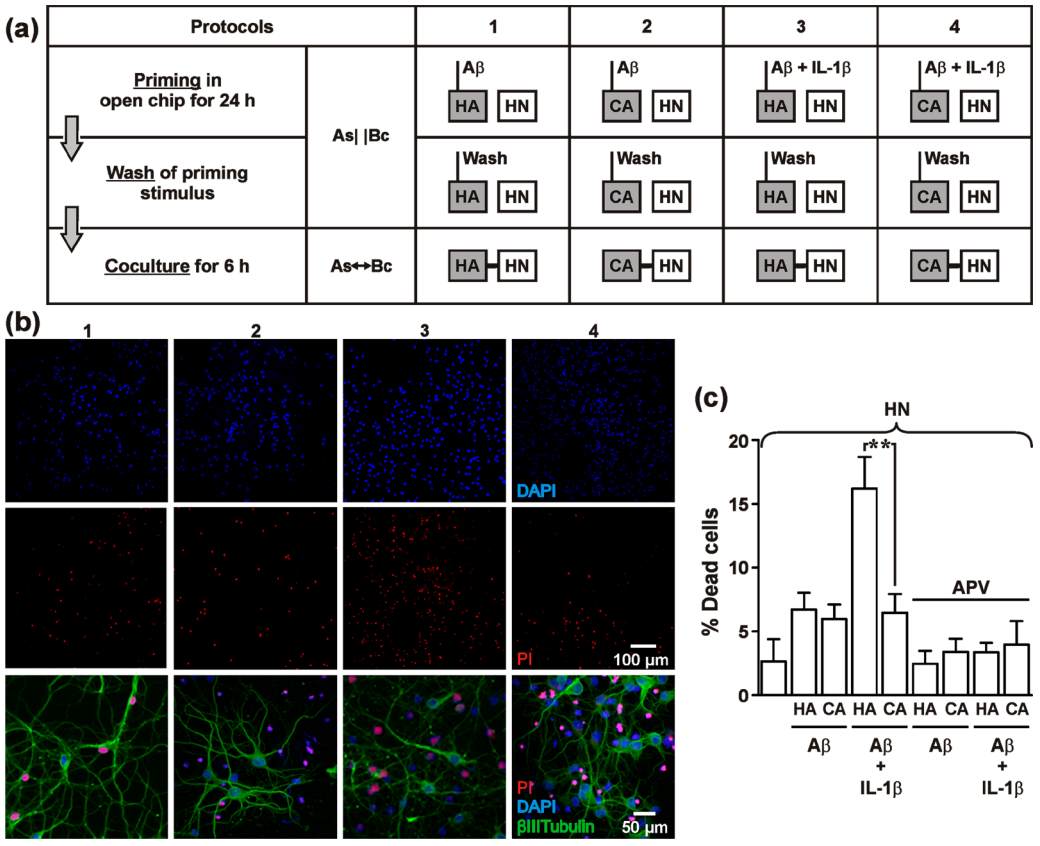

Figure 3. Role of hippocampal (HAs) and cortical (CAs) astrocytes on neuronal viability in the context of Aβ insult. (a) Protocols involved HNs that were cocultured with either CAs or HAs, previously primed with Aβ or with Aβ + IL-1β. (b) Representative vitality images showing DAPI (blue)/PI (red) and βIII tubulin (green) staining of HNs from the four protocols described in panel a. (c) Comparison of death rates of HNs (unlabeled bar). HNs in microfluidic communication with HAs show a significant increase of cell death. This is not observable when HNs are cocultured with CAs. The detrimental effect, which primed HAs have on HNs, seems to relate to glutamate excitotoxicity because the presence of APV significantly reduces cell death.

develop normally and form wide networks of cells connected by synaptic contacts, as revealed by immunocytochemical staining with βIII tubulin (Figure 1b). The ability of neurons plated on oMFN to form synaptic contacts (sites of communication among neurons) is demonstrated by immunocytochemical staining for the synaptic vesicle glutamate transporter vGlut, which labels presynaptic boutons (Figure 1b, arrowheads). Quantitative evaluation of intracellular calcium concentrations shows basal intracellular calcium levels comparable to neurons maintained under standard culturing conditions on poly-L-lysine-coated glass (F340/380; glass, 0.69 + 0.04; PDMS, 0.56 + 0.03; n = 20, p = 0.35, Student's t test) and a similar amplitude of the peak response following exposure to depolarizing stimuli with 50 mM KCl (F340/380; glass, 0.14 + 0.01; PDMS, 0.15 + 0.01; cells number = 15, three independent experiments, Student's t test). Furthermore, HNs grown on glass or oMFNs show comparable amplitude (pA; glass, 92.67 + 10.01; PDMS, 105.97 + 15.45; cells number = 10, three independent experiments, p = 0.26, Student's t test) and frequency (Hz; glass, 2.74 + 0.58; PDMS, 2.41 + 0.73; cells number = 10, three independent experiments, p = 0.97, Student's t test) of miniature excitatory postsynaptic currents (mEPSCs) recorded using whole-cell patch-clamp. These data indicate that primary neuronal cultures from rat hippocampus grown on oMFNs exhibit morphological, functional, and electrophysiological properties similar to those of neurons grown in standard culturing conditions on glass coverslips; hence, growth of cultures in the cell chambers of the chip neither influences neuronal viability nor the overall cellular phenotype and development.

Hippocampal or Cortical Astrocytes Differently Protect Hippocampal Neurons during Ischemic Insult. We interrogated the contribution of specific cell types to neuroinflammatory events that lead to neuronal degeneration in a well-characterized in vitro model of ischemia, namely, oxygen–glucose deprivation (OGD) protocol.[17] To this end, primary HNs were grown in chamber B, while either cortical (CA) or hippocampal (HA) astrocytes were grown in chamber A (Figure 2a). Cells were either cultured independently (Figure 2a, protocols 1 and 2) or kept in microfluidic communication (Figure 2a, protocols 3 and 4) in open microfluidic setting. Within these protocols, cells in the different oMFN chips were maintained either in standard culturing conditions (Ac, Bc) or challenged with the OGD protocol (As, Bs). After 2 h of OGD, cells were allowed to recover for 24 h before being subjected to viability assays. The quantitative evaluation of cell viability, expressed as ratio of propidium iodide (PI) positive cells to the total number of cells (Figure 2b, nuclear DAPI staining, blue; PI, red) revealed that, whereas astrocytes (HA, CA) remain largely viable after the OGD challenge (PI/DAPI%: CA = 0.60 + 0.12%; HA = 2.24 + 0.77%), neurons (HN) maintained in isolation display a significant percentage of PI positive cells (19.18 + 4.65%, p < 0.01, Figure 2c). Notably, OGD challenge of HNs maintained in microfluidic communication with CAs

dx.doi.org/10.1021/ac302094z | Anal. Chem. XXXX, XXX, XXX–XXX

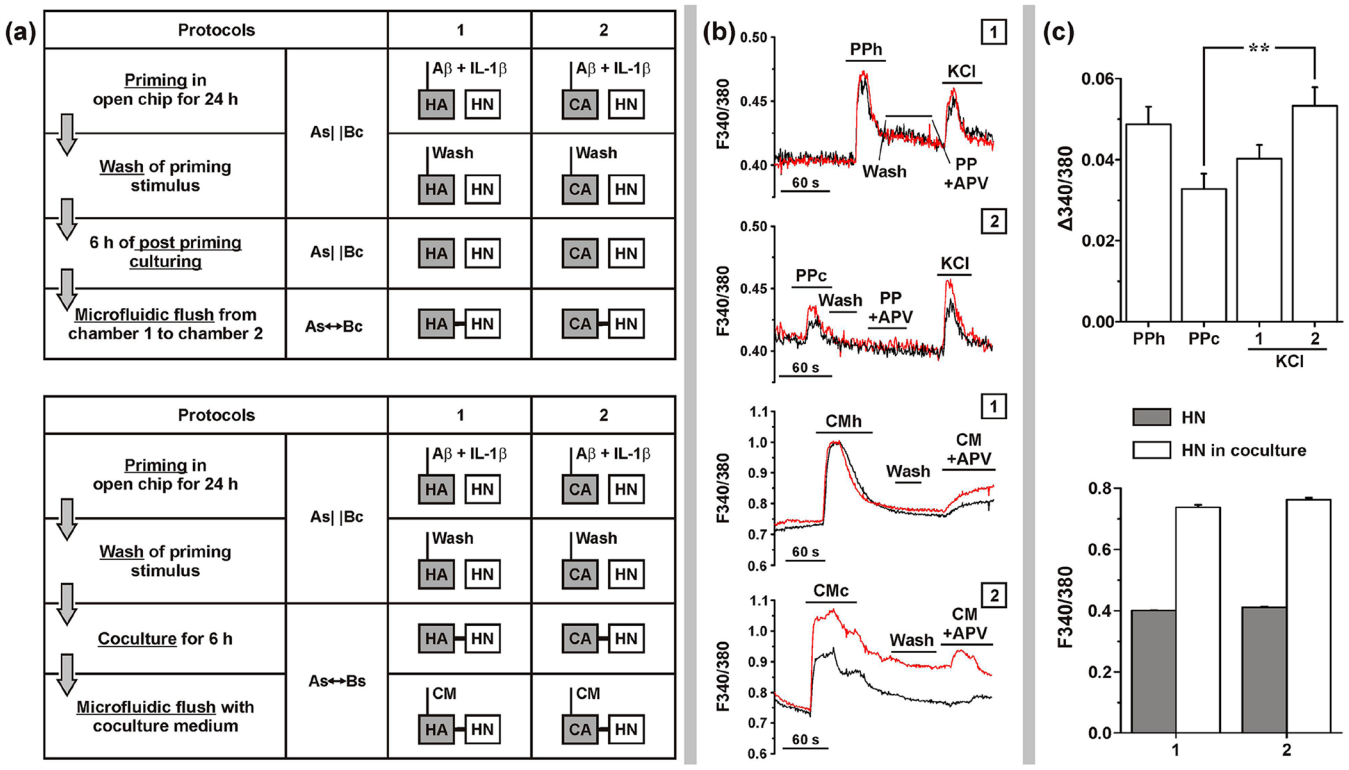

Figure 4. (a) Representation of the experiments in which hippocampal (HAs, protocol 1) and cortical (CAs, protocol 2) astrocytes are primed with Aβ + IL-1β and then either further cultured independently (upper panel) or immediately put into microfluidic communication with HNs (lower panel). (b) Two representative traces showing single-cell ratiometric calcium acquisitions of HNs in chamber B exposed to glial-conditioned medium from chamber A coming either from independent culturing (upper panel) or immediate microfluidic communication (lower panel) (PPh = postpriming medium from HAs; PPc = postpriming medium from CAs; CMh = coculture medium from HAs; CMc = coculture medium from CAs). (c) Quantification of either cell calcium influx in HNs following exposure to glial-conditioned medium either from HAs (PPh) or CAs (PPc) with respect to biochemical depolarization by exposure to 50 mM KCl (upper panel) and quantification of basal intracellular calcium levels in HNs cultured either independently or in microfluidic communication with either HAs (1) or CAs (2) primed with Aβ + IL-1β (lower panel).

results in a significant reduction of PI positive cells (2.90 + 2.08%, cells number = 30, three independent experiments, $p < 0.01$) with respect to neurons maintained in microfluidic communication with HAs (19.58 + 3.80%, cells number = 30, three independent experiments $p = 0.95$, analysis of variance (ANOVA), post hoc Tukey's method), suggesting a neuroprotective role played by CAs, but not by HAs.

Hippocampal or Cortical Astrocytes Differently Affect Neuronal Viability during Aβ Insult. To address whether the different effect on the neuronal viability exerted by astrocytes derived from different brain regions is limited to conditions of ischemic insult, we employed oMFNs to dissect cell-specific contributions in another neuroinflammatory context, namely, the exposure of brain cells to amyloid β fibrils. HNs were grown in chamber B, while either CAs or HAs were grown in chamber A (Figure 3a) in open microfluidic setting. CAs and HAs in chamber A were independently exposed during 24 h to either Aβ alone or to Aβ + the proinflammatory cytokine IL-1β (Figure 3a), washed, and put into closed microfluidic communication for 6 h with HNs (chamber B). HAs, CAs, and HNs independently challenged with either Aβ or Aβ + IL-1β do not show significant cell death (HN = 2.65 + 1.72; HA = 6.71 + 1.33; CA = 5.97 + 1.12; cells number = 15 , three independent experiments, post hoc Tukey's method). Also, HNs, put into closed microfluidic communication for 6 h with CAs and HAs, previously primed only with Aβ or IL-1β, show only a moderate increase in neuronal death (data not shown), thus confirming the previously reported observation that IL-1β or Aβ fibrils alone do not heavily impact neuronal viability.[18] However, when HNs were put into closed microfluidic communication with HAs previously challenged with Aβ + IL-1β, a significant increase in cell death was detected (Figure 3b, HN = 16.20 + 2.44; cells number = 15; three independent experiments, $p < 0.01$, post hoc Dunnett's method), which was not observed in HNs cocultured with CAs under the same conditions (Figure 3c, HN = 6.48 + 1.47; cells number = 15; three independent experiments, $p = 0.35$, post hoc Tukey's method). The harmful effect of HAs on HNs following exposure to Aβ + IL-1β was abolished in the presence of APV, a selective antagonist of NMDA receptors (Figure 3c).

To address whether HN damage may result from the release of soluble mediators by HAs when exposed to Aβ + IL-1β, we took advantage of the possibility to close the oMFN lid and flush the cells in chamber B with the medium from chamber A, while monitoring cellular response using single-cell calcium imaging. Astroglial cells, either HAs or CAs, independently cultured in chamber A of open oMFNs, were then primed with Aβ + IL-1β for 24 h, washed, and further cultured for 6 h (Figure 4a). Subsequently, the chambers were put into microfluidic communication using the closed microfluidic setting, and intracellular calcium dynamics of HNs in chamber 2 were acquired by time-lapse ratiometric single-cell calcium imaging acquisitions (Figure 4b). A quantitative analysis of the response of HNs to either HA postpriming medium (PPh) or CA postpriming medium (PPc) was then carried out. Figure 4c

dx.doi.org/10.1021/ac302094z | Anal. Chem. XXXX, XXX, XXX−XXX

shows that HNs challenged with PPh exhibit higher calcium transients compared to HNs exposed to PPc. Neurons in both chambers show higher basal intracellular calcium levels when in microfluidic communication (Figure 4c, lower panel), but respond similarly to 50 mM KCl stimulation, thus excluding a different intrinsic neuronal responsiveness to depolarization (Figure 4c, upper panel). In both cases, the calcium elevation produced by the postpriming solution was blocked by the NMDA receptor blocker APV (Figure 4b).

DISCUSSION

The analytical method shown here uses microfluidic networks in open and closed configurations to investigate the role played by astrocytes derived from different regions of the brain in controlling neuronal viability under two types of insults, ischemic insult and exposure to Aβ + IL-1β. In both situations, a clear difference was found between hippocampal and cortical astrocytes, with hippocampal astrocytes failing in supporting neurons after ischemic insult and playing a more detrimental role on neurons after exposure to Aβ + IL-1β.

Although astrocytes throughout the central nervous system share many common traits, a marked phenotypic diversity is detectable among astrocytes from different brain regions.[19] Heterogeneity includes the different types and levels of neuropeptides and receptors and the specific expression of membrane transporters and channels.[20−26] These phenotypic differences result in functional heterogeneity among cortical and hippocampal astrocytes which results in specific functional features,[27−29] for example, in an increased glutamate uptake capability by cortical rather than hippocampal astrocytes following injury.[19,30−32]

Although ample data suggest that astrocytes play a role in both the initiation and propagation of ischemic injury, the contribution of specific astrocyte populations to this process has never been defined. Astrocytes are the principal housekeeping cells of the nervous system, playing multiple supportive tasks for neurons, including reuptake of neurotransmitters released during synaptic activity, control of ion homeostasis and release of neurotrophic factors, shuttling of metabolites and waste products, and participation in the formation of the blood−brain barrier.[33] Failure of any of these supportive functions of astrocytes can represent a threat for neuronal survival.[34] Evidence is suggesting that astrocytes and factors released by astrocytes are differently modulating neuronal functionality according to regional localization and concentration of chemical mediators.[17] In particular, it has been shown that hippocampal astrocytes are more sensitive than cortical astrocytes to OGD stimulation, resulting in an increased hippocampal release of LDH, although reasons for the observed difference have to date not been determined.[20] By indicating a selective neuroprotective action of CAs—but not of HAs—upon OGD challenge, our data suggest regional differences in astrocyte ability to support neuronal metabolic needs under ischemic insult. This is likely to result from different astroglial vulnerability to ischemia, due to both a minor metabolic suffering of CAs[35] and a higher sensibility of HAs to reactive oxygen species.[36]

A primary role of astrocytes in control of neuronal viability has also been demonstrated in neurodegenerative disorders, such as Alzheimer's disease (AD), in which neuroinflammatory events are heavily involved. The main inflammatory players in AD are the glial cells which initiate the inflammatory response. Indeed one of the earliest neuropathological changes in AD is the accumulation of astrocytes at sites of Aβ deposition. Several lines of evidence suggest that neurons are damaged by neurotoxic molecules elaborated from glial activation, and indeed Aβ induces inflammatory mediators, such as cyclooxygenase 2 (COX-2), inducible nitric oxide synthase (iNOS), IL-1β, and tumor necrosis factor α.[37−45]

Our data indicate that astrocytes from different brain regions differently affect neuronal viability upon exposure to inflammatory stimulus Aβ + IL-1β, with HAs contributing more heavily to neuronal death than CAs. The harmful effect of HAs could presumably be mediated by the higher levels of glutamate accumulated in the hippocampal relative to cortical astrocyte medium upon stimulus challenge, given that neuronal death is prevented by the NMDA blocker APV. However, it is very likely that also other inflammatory mediators contribute to the process.

CONCLUDING REMARKS

Dissecting the interactions between cell populations using a flexible microfluidic format and various signal readouts is a powerful method for investigating the specific dynamics of molecular mechanisms involved in the crosstalk among different cell populations during neuroinflammatory events. By the combined action of morphological and functional analysis on primary cell cultures, either cultured independently or in microfluidic communication, we were able to distinguish brain-region-specific glial contribution in two different in vitro models of neuroinflammation, presumably because of a glutamate-mediated excitoxicity caused by a region-dependent alteration of metabolic activity. We suggest oMFNs and the method shown here to be a valuable, versatile, and flexible analytical solution to unravel how different cell types of the brain contribute to the crosstalk events leading to neurodegeneration.

MATERIALS AND METHODS

oMFNs Fabrication and Setup. oMFNs were fabricated by casting PDMS (Sylgard 184, Dow Corning, Midland, MI) onto microstructured 4 in. Si wafers (Siltronix, Geneva, Switzerland) used as molds. These Si molds were made using standard photolithography (64 000 dpi polymer masks, Zitzmann GmbH, Germany) and deep reactive ion etching (STS ICP, Surface Technology Systems, U.K.). The Si molds were coated with a fluorinated material (1*H*,1*H*,2*H*,2*H*-perfluorodecyltrichlorosilane from ABCR GmbH, Karlsruhe) at the end of the etching process for better release of the PDMS after curing overnight at 60 °C. To this end, the Si molds were cleaned using an oxygen-based plasma, exposed to vapors of the fluorinated silane using a desiccator (50−100 mbar and 30 min of exposure time), and baked 2 h at 80 °C. The PDMS oMFNs with 150 μm deep structures were separated using a scalpel and stored in a plastic dish until used.

The Si lids were fabricated using similar lithography and etching processes as for the Si molds. NanoPort assemblies (Upchurch Scientific, Ercatech, Switzerland) were mounted to the backside of the lids, in alignment with the vias for liquid connection.

Prior to the seeding of cells, the oMFNs were treated with an oxygen-based plasma for 30 s (Technics Plasma 100-E, Florence, KY) at 200 W of coil power and then coated with a 0.5 mg mL^{-1} solution of poly-L-lysine. The oMFNs were incubated with the poly-L-lysine overnight at room temper-

dx.doi.org/10.1021/ac302094z | Anal. Chem. XXXX, XXX, XXX−XXX

ature. After a washing step with PBS and water, the oMFNs were dried under a stream of N_2, and cell suspensions were added onto the chambers. This was done by placing ~750 cells mm^{-2} in each chamber of an oMFN. The oMFN was then placed in a Petri dish with a few milliliters of water next to it to prevent evaporation of the liquid in the cell chambers. The Petri dish with the oMFN was then kept in an incubator for up to 10 days. If necessary, a replacement of growth medium during incubation was done using a pipet.

The tubing and fittings needed for microfluidic experiments were purchased from Upchurch Scientific. Active pumping of liquids was done using high-precision syringe pumps (Cetoni GmbH, Korbussen, Germany), which were equipped with 50 μL glass syringes (Hamilton, Bonaduz, Switzerland). A custom-made aluminum holder facilitated the assembly of the oMFN with the lid. During this procedure, the lid was normally connected to prefilled tubing to prevent air bubble formation in closed oMFNs.

Chemicals and Biomolecules. Antibodies against βIII tubulin (cat. no. G712A, 1:300 dilution) were from Promega (Milano, Italy). $A\beta_{1-42}$ (cat. no. 24224, 1 μM) was from Anaspect (Fremont, CA); DAPI and Fura-2 AM were from Invitrogen (Milano, Italy). Propidium iodide (20 ng mL^{-1}), Abs against GFAP (1:100 dilution) and IB4 (1:200 dilution), and KCl were purchased from Sigma-Aldrich (Milano, Italy); IL-1β was from Peprotech (DBA, Italy), and APV was from Tocris (Bristol, U.K.). Vglut (cat. no. 135311, 1:1000 dilution) was purchased from Synaptic Systems (Goettingen, Germany).

Primary Cultures of Hippocampal/Cortical Neurons and Astrocytes. Primary neuronal cultures were prepared from the brains of 18 day old rat embryos (Charles River, Milan, Italy) as previously described[3] with minor modifications. Briefly, the hippocampi or cortices were isolated from total brain, incubated with trypsin at 37 °C, and then dissociated to obtain separated cells, which were then plated at a density of ~750 cells mm^{-2} in each chamber of the chip and grown in neurobasal medium supplemented with B27, 0.5 mM glutamine, and 12.5 μM glutamate. Hippocampal/cortical astrocytic cultures from rat pups (P2) were obtained using previously described methods.[3] Briefly, after dissection, the hippocampi/cortices were dissociated by treatment with trypsin (0.25% for 10 min at 37 °C) followed by fragmentation with a fire-polished Pasteur pipet. The dissociated cells were cultured for 14 days, trypsinized, and plated in a cell chamber at a density of 2000 cells/chamber, and the cultures were grown in minimum essential medium (Invitrogen, Italy) supplemented with 20% fetal bovine serum (Euroclone Ltd., U.K.) and glucose at a final concentration of 5.5 g L^{-1}. Prior to trypsinization, astrocytes were shaken as previously described[3] in order to detach microglia cells. Cell purity of astrocytic culture on PDMS was confirmed by positivity to immunocytochemical staining with glial fibrillar acidic protein GFAP and lack of signal to microglia marker IB4 as previously reported.[16]

Immunocytochemical Staining. Primary cells, both neurons and astrocytes, were fixed in 4% paraformaldehyde and 4% sucrose at room temperature (RT) for 10 min. Primary and secondary antibodies were applied in GDB buffer (30 mM phosphate buffer, pH 7.4, containing 0.2% gelatin, 0.5% Triton X-100, and 0.8 M NaCl) for 2 h at RT or overnight at 4 °C. The confocal images were acquired with a Leica SPE confocal microscope, using a Nikon (Tokyo, Japan) 40× objective. Each image was a *z*-series projection taken at 0.8 μm depth intervals.

Preparation of Fibrillar Aβ and Cells Treatment. Fibrillar $A\beta_{1-42}$ was prepared as previously described[30] by incubating freshly solubilized peptides at 50 μM in sterile water for 5 days at 37 °C. CAs and HAs were stimulated with fibrillar $A\beta_{1-42}$ (1 μM) alone or combined to IL-1β (10 nM). After 24 h, the cells were washed with Krebs−Ringer solution, fresh neuronal medium was added, and the cells were placed in coculture with HNs for 6 h.

OGD Protocol. To mimic ischemic condition in vitro, cells were exposed to OGD following published methods.[44,45] Culture medium was replaced with a solution containing 130 mM NaCl, 5 mM KCl, 2 mM $CaCl_2$, 1.2 mM $MgSO_4$, 1.2 mM KH_2PO_4, and 25 mM 4-(2-hydroxyethyl)piperazine-1-ethanesulfonic acid (HEPES). Culture plates were placed in an airtight chamber (Billups-Rothenberg, Del Mar, CA, U.S.A.). The chamber was flushed with 95% N_2/5% CO_2 for 5 min with 20 L min^{-1} gas flow, sealed, and placed in a 37 °C incubator for the appropriate duration. After the insult, OGD media were replaced with neuronal complete medium, and the cultures were returned to a normoxic environment. To examine the effects of reperfusion, cells were analyzed either immediately or after 24 h of recovery.

Quantitative Evaluation of Intracellular Calcium Dynamics. Cultures were loaded for 35−40 min at 37 °C with 2 μM Fura-2 AM in Krebs−Ringer solution buffered with HEPES, 125 mM NaCl, 5 mM KCl, 1.2 mM $MgSO_4$, 2 mM $CaCl_2$, 10 mM glucose, and 25 mM HEPES (pH 7.4) and were washed twice with prewarmed Krebs−Ringer solution before recordings were made. The recording setup comprised an inverted microscope (Axiovert 100, Zeiss, Germany) equipped with a Ca^{2+} imaging unit. Polychrome IV (TILL Photonics, Germany) was used as a light source. Fura-2 fluorescence images were collected with a PCO Super VGA SensiCam (Axon Instruments, CA, U.S.A.) at 25 °C and analyzed with TILL Vision Software (TILL Photonics, Germany). Single-cell 340/380 nm fluorescence ratios, acquired at a sampling frequency of 1−4 s^{-1}, were analyzed with Origin 6.0 (Microcal Software Inc., MA, U.S.A.).

Electrophysiological Recordings. Whole-cell voltage-clamp recordings of spontaneous synaptic activity were performed on rat embryonic HNs maintained in culture for 10−14 DIV. Patch pipettes (2−4 MΩ) were pulled using a micropipet electrode puller (Sutter Instruments) and filled with internal recording solution containing (in mM) KGluc 130, EGTA 1, KCl 10, $MgCl_2$ 2, HEPES 10, Mg ATP 40, Tris−GTP 3 (pH 7.3). The cells plated on glass coverslips or in cell chambers of microfluidic chips were placed in a recording chamber perfused continuously with extracellular solution containing (in mM) NaCl 125, KCl 5, $MgSO_4$ 1.2, $CaCl_2$ 2, $KHPO_4$ 1.2, HEPES 25, Glu 6 (pH 7.3). Recordings were conducted at −70 mV. The series resistance ranged from 10 to 20 MΩ and was monitored for consistency during recordings. Cells in culture with leak currents >100 pA were excluded from our analysis. Signals were recorded using Multiclamp 700B amplifiers and digitized with Digidata 1440 (Axon Instruments, Molecular Devices). Signals were amplified, sampled at 10 kHz, filtered to 2 or 5 kHz, and analyzed using the pClamp 10 data acquisition and analysis program.

Data Analysis. The data are presented as means ± SE. Statistical significance was evaluated by the Student's *t* test or one-way ANOVA. Differences were considered significant if $p = 0.05$ and are indicated by an asterisk in all figures, whereas those at $p < 0.01$ are indicated by double asterisks.

dx.doi.org/10.1021/ac302094z | Anal. Chem. XXXX, XXX, XXX−XXX

AUTHOR INFORMATION

Corresponding Author

*Phone: +39-02-56660156. E-mail: fabio.bianco@neuro-zone.com.

Author Contributions

¶These authors contributed equally to this work.

Notes

The authors declare the following competing financial interest(s): the publication can have an impact on the group's rating in the companies at the end of the year. This can influence salaries (bonus, salary increase etc.).

ACKNOWLEDGMENTS

We thank R. Stutz for his help with the fabrication of molds and chips, M. Hitzbleck, G. V. Kaigala, and C. Verderio for discussions, and W. Riess, M. Despont, and V. Vogel (ETHZ) for their continuous support. This work was partially supported by MIUR art. 11 D.M. no. 593/2000 to M.M. and F.B., by CARIPLO 2008-3184 to M.M., and by the European Union Seventh Framework Program under Grant Agreement No. HEALTH-F2-2009-241498 ("EUROSPIN" project) to M.M.

REFERENCES

(1) Golde, T. E. *Mol. Neurodegener.* **2009**, *4*, 4−8.
(2) Glass, C. K.; Saijo, K.; Winner, B.; Marchetto, M. C.; Gage, F. H. *Cell* **2012**, *19*, 918−934.
(3) Bianco, F.; Pravettoni, E.; Colombo, A.; Schenk, U.; Moller, T.; Matteoli, M.; Verderio, C. *J. Immunol.* **2005**, *174*, 7268−7277.
(4) Agostinho, P.; Cunha, R. A.; Oliveira, C. *Curr. Pharm. Des.* **2010**, *16*, 2766−2778.
(5) Salmina, A. B. *J. Alzheimer's Dis.* **2009**, *16*, 485−502.
(6) El-Ali, J.; Sorger, P. K.; Jensen, K. F. *Nature* **2006**, *27*, 403−411.
(7) Cooksey, G. A.; Sip, C. G.; Folch, A. *Lab Chip* **2009**, *9*, 417−426.
(8) Nilsson, J.; Evander, M.; Hammarström, B.; Laurell, T. *Anal. Chim. Acta* **2009**, *649*, 141−157.
(9) Lovchik, R. D.; Bianco, F.; Matteoli, M.; Delamarche, E *Lab Chip* **2009**, *9*, 1395−1402.
(10) Taylor, A. M.; Rhee, S. W.; Tu, C. H.; Cribbs, D. H.; Cotman, C. W.; Jeon, N. J. *Langmuir* **2003**, *19*, 1551−1556.
(11) Futai, N.; Gu, W.; Song, J. W.; Takayama, S. *Lab Chip* **2006**, *6*, 149−154.
(12) Lovchik, R. D.; Bianco, F.; Tonna, N.; Ruiz, A.; Matteoli, M.; Delamarche, E. *Anal. Chem.* **2010**, *82*, 3936−3942.
(13) Hsu, C.-H.; Chen, C.; Folch, A. *Lab Chip* **2004**, *4*, 420−424.
(14) Sung, J. H.; Kam, C.; Shuler, M. L. *Lab Chip* **2012**, *10*, 446−455.
(15) Wu, H.-I.; Cheng, G.-H.; Wong, Y.-Y.; Lin, C.-M.; Fang, W.; Chow, W.-Y.; Chang, Y.-C. *Lab Chip* **2010**, *10*, 647−653.
(16) Lovchik, R. D.; Tonna, N.; Bianco, F.; Matteoli, M.; Delamarche, E. *Biomed. Microdevices* **2010**, *12*, 275−282.
(17) Lin, C. H.; Chen, P. S.; Gean, P. W. *Eur. J. Pharmacol.* **2008**, *589*, 85−93.
(18) Tan, J.; Town, T.; Saxe, M.; Paris, D.; Wu, Y.; Mullan, M. *J. Immunol.* **1999**, *163*, 6614−6621.
(19) Han, B. C.; Koh, S. B.; Lee, E. Y.; Seong, Y. H. *Life Sci.* **2004**, *76*, 573−583.
(20) Lee, Y. S.; Ouyang, Y. B.; Giffard, R. G. *FEBS Lett.* **2006**, *580*, 4865−4871.
(21) Venance, L.; Prémont, J.; Glowinski, J.; Giaume, C. *J. Physiol.* **1998**, *510*, 429−440.
(22) McCarthy, K. D.; Salm, A. K. *Neuroscience* **1991**, *41*, 325−333.
(23) Sharif, A.; Duhem-Tonnelle, V.; Allet, C.; Baroncini, M.; Loyens, A.; Kerr-Conte, J.; Collier, F.; Blond, S.; Ojeda, S. R.; Junier, M. P.; Prevot, V. *Glia* **2009**, *57*, 362−379.
(24) Shinoda, H.; Marini, A. M.; Cosi, C.; Schwartz, J. P. *Science* **1989**, *245*, 415−417.
(25) Olsen, M. L.; Campbell, S. L.; Sontheimer, H. *J. Neurophysiol.* **2007**, *98*, 786−793.
(26) Oberheim, N. A.; Goldman, S. A.; Nedergaard, M. *Methods Mol. Biol.* **2012**, *814*, 23−45.
(27) McKhann, G. M.; D'Ambrosio, R.; Janigro, D. *J. Neurosci.* **1997**, *17*, 6850−6863.
(28) Matthias, K.; Kirchhoff, F.; Seifert, G.; Hüttmann, K.; Matyash, M.; Kettenmann, H.; Steinhäuser, C. *J. Neurosci.* **2003**, *23*, 1750−1758.
(29) Poopalasundaram, S.; Knott, C.; Shamotienko, O. G.; Foran, P. G.; Dolly, J. O.; Ghiani, C. A.; Gallo, V.; Wilkin, G. P.; Ralay Ranaivo, H.; Craft, J. M.; Hu, W.; Guo, L.; Wing, L. K.; Van Eldik, L. J.; Watterson, D. M. *J. Neurosci.* **2006**, *26*, 662−670.
(30) Morga, E.; Faber, C.; Heuschling, P. *J. Neuroimmunol.* **1998**, *87*, 179−184.
(31) Kipp, M.; Norkute, A.; Johann, S.; Lorenz, L.; Braun, A.; Hieble, A.; Gingele, S.; Pott, F.; Richter, J.; Beyer, C. *J. Mol. Neurosci.* **2008**, *35*, 35−43.
(32) Fitting, S.; Zou, S.; Chen, W.; Vo, P.; Hauser, K. F.; Knapp, P. E. *J. Proteome Res.* **2010**, *9*, 1795−1804.
(33) Volterra, A.; Meldolesi, J. *Nat. Rev. Neurosci.* **2005**, *6*, 626−640.
(34) Takano, T.; Oberheim, N.; Cotrina, M. L.; Nedergaard, M. *Stroke* **2009**, *40*, 8−12.
(35) Zhao, G.; Flavin, M. P. *Neurosci. Lett.* **2000**, *285*, 177−180.
(36) Silva, G. A.; Feeney, C.; Mills, L. R.; Theriault, E. *Eur. J. Neurosci. Methods* **1998**, *80*, 75−79.
(37) Valles, S. L.; Dolz-Gaiton, P.; Gambini, J.; Borras, C.; Lloret, A.; Pallardo, F. V.; Viña, J. *Brain Res.* **2010**, *1312*, 138−144.
(38) Meda, L.; Cassatella, M. A.; Szendrei, G. I.; Otvos, L.; Baron, P.; Villalba, M.; Ferrari, D.; Rossi, F. *Nature* **1995**, *374*, 647−650.
(39) Tan, K. H.; Purcell, W. M.; Heales, S. J.; McLeod, J. D.; Hurst, R. D. *NeuroReport* **2002**, *13*, 2587−2591.
(40) Jana, A.; Pahan, K. *J. Neurosci.* **2010**, *30*, 12676−12689.
(41) Ralay Ranaivo, H.; Craft, J. M.; Hu, W.; Guo, L.; Wing, L. K.; Van Eldik, L. J.; Watterson, D. M. *J. Neurosci.* **2006**, *26*, 662−670.
(42) Brewer, G. J.; Torricelli, J. R.; Evege, E. K.; Price, P. J. *J. Neurosci. Res.* **1993**, *35*, 567−576.
(43) Calegari, F.; Coco, S.; Taverna, E.; Bassetti, M.; Verderio, C.; Corradi, N.; Matteoli, M.; Rosa, P. *J. Biol. Chem.* **1999**, *274*, 22539−22547.
(44) Romera, C.; Hurtado, O.; Botella, S. H.; Lizasoain, I.; Cárdenas, A.; Fernández-Tomé, P.; Leza, J. C.; Lorenzo, P.; Moro, M. A. *J. Neurosci.* **2004**, *24*, 1350−1357.
(45) Goldberg, M. P.; Choi, D. W. *J. Neurosci.* **1993**, *13*, 3510−3524.